

Article

Asymmetric and Reduced Xanthene Fluorophores: Synthesis, Photochemical Properties, and Application to Activatable Fluorescent Probes for Detection of Nitroreductase

Kunal N. More ^{1,†} , Tae-Hwan Lim ^{1,†}, Julie Kang ¹, Hwayoung Yun ² , Sung-Tae Yee ¹ and Dong-Jo Chang ^{1,*} 

¹ College of Pharmacy and Research Institute of Life and Pharmaceutical Sciences, Suncheon National University, Suncheon 57922, Korea

² College of Pharmacy, Pusan National University, Busan 46241, Korea

* Correspondence: djchang@scnu.ac.kr; Tel.: +82-61-750-3765

† These two authors contributed equally to this work.

Academic Editor: David Díez

Received: 21 August 2019; Accepted: 2 September 2019; Published: 3 September 2019



Abstract: Xanthene fluorophores, including fluorescein, rhodol, and rhodamines, are representative classes of fluorescent probes that have been applied in the detection and visualization of biomolecules. “Turn on” activatable fluorescent probes, that can be turned on in response to enzymatic reactions, have been developed and prepared to reduce the high background signal of “always-on” fluorescent probes. However, the development of activity-based fluorescent probes for biological applications, using simple xanthene dyes, is hampered by their inefficient synthetic methods and the difficulty of chemical modifications. We have, thus, developed a highly efficient, versatile synthetic route to developing chemically more stable reduced xanthene fluorophores, based on fluorescein, rhodol, and rhodamine via continuous Pd-catalyzed cross-coupling. Their fluorescent nature was evaluated by monitoring fluorescence with variation in the concentration, pH, and solvent. As an application to activatable fluorescent probe, nitroreductase (NTR)-responsive fluorescent probes were also developed using the reduced xanthene fluorophores, and their fluorogenic properties were evaluated.

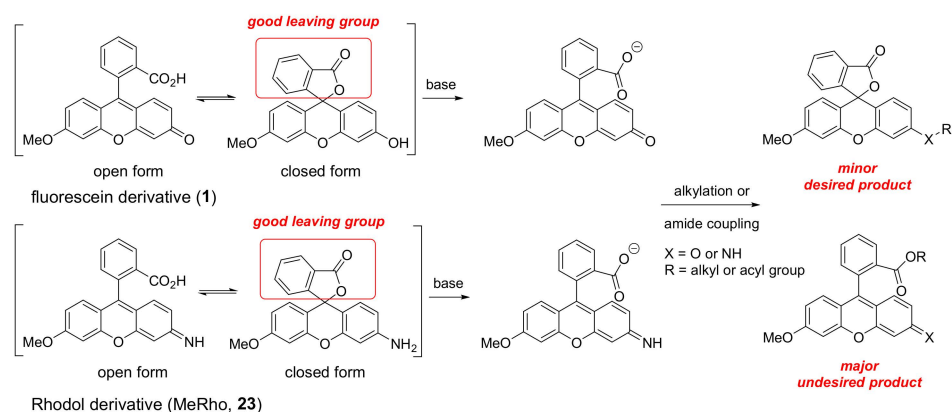
Keywords: fluorescence; xanthene fluorophore; reduced rhodafluor; activatable fluorescent probe; nitroreductase

1. Introduction

The xanthene scaffold-based fluorophores, including fluorescein, rhodamine, and their hybrid structure (rhodol), are among the most commonly used fluorophores, which have been widely applied as fluorescent probes to detect various biological and cellular processes [1,2]. Rhodol and rhodamine fluorophores in the form of activity-based fluorescent probes have attracted much interest, due to their high quantum yields in aqueous solutions, over a broad pH range and better photostability, as compared to fluorescein in detecting various cellular phenomena [3]. Previously, fluorescent probes carrying macromolecules or small-molecule ligands for targeted delivery have been developed and used in biomedical imaging. These fluorescent probes are disadvantageous, due to their “always-on” nature for imaging which lead to poor target-to-background ratios, that result from non-specific binding. Activatable “turn-on” fluorescent probes were assisted in overcoming this drawback, as they emit fluorescence only under specific conditions, such as binding to the target protein [1,4,5]. Our research group has attempted the development of nitroreductase-responsive fluorescent probes for hypoxia imaging, based on xanthene fluorophores, such as fluorescein and rhodol fluorophores, which bear a

carboxylate group [6]. However, the selective functionalization of the terminal -OH or -NH₂ group on the xantheno ring via alkylation or amide coupling is difficult, because carboxylate is a good leaving group (Figure 1A). Alkylation or amide coupling of typical xantheno fluorophores mainly produce an undesired product via a reaction of the carboxylate group in its open form, and leads to low yield of the desired product. We envisioned that alkylation or amide coupling could be achieved at the desired position by shifting the equilibrium toward closed form (Figure 1B). Reduced xantheno fluorophores have a benzyl alkoxy group, which is a poorer leaving group, compared to the carboxylate group in typical xantheno fluorophores. Koide's group first reported a reduced fluorescein derivative, containing a benzyl alcohol, instead of benzoic acid, producing Pittsburgh green, and it was capable of detecting palladium and mercury [7,8]. Urano's group also reported various reduced xantheno fluorophores, based on rhodol and rhodamine containing benzyl alcohol (HMDER), benzyl thiol, and benzyl amine instead of the benzoic acid, and designed a novel activatable fluorescent probe, using HMDER for *in vitro* and *in vivo* imaging of β -galactosidase [9–12]. Subsequently, a few activatable fluorescent probes, based on reduced rhodafuors for biomedical imaging or sensing ozone, have been reported [13–22].

A. Alkylation and amide coupling reactions of typical fluorescein and rhodol fluorophores



B. Equilibrium between non-fluorescent closed form and fluorescent open form in xantheno fluorophores

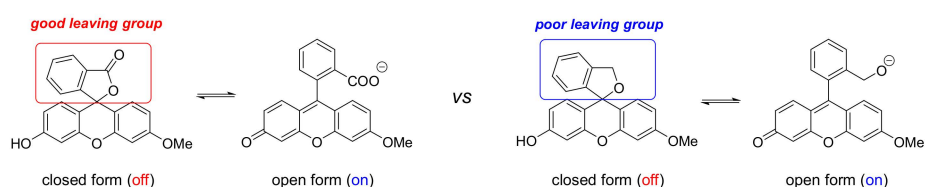
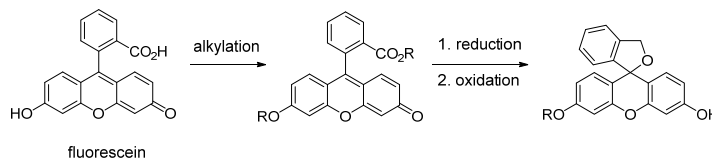


Figure 1. Structural analysis of typical and reduced xantheno fluorophores. (A) Reactivity of fluorescein and rhodol derivatives in alkylation and amide coupling reactions; and (B) equilibrium between closed and open forms affecting fluorescence.

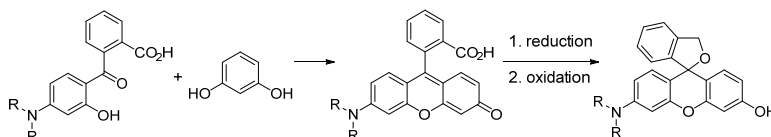
Asymmetric and reduced xantheno fluorophores based on fluorescein can be synthesized from commercially available fluorescein via the reduction and subsequent oxidation of the carboxylate group of fluorescein (Figure 2A), whereas reduced rhodol and rhodamine fluorophores can be prepared by a convergent synthesis of the xantheno moiety via the reaction of 2-(4-(dialkylamino)-2-hydroxybenzoyl)benzoic acid with resorcinol or 4-aminophenol, followed by reduction and subsequent oxidation (Figure 2B,C) [9–11,14,23]. However, the current synthetic methods have limitations in effectively generating diverse asymmetric and reduced xantheno fluorophores. Not only different types of fluorophores, such as fluorescein, rhodol, and rhodamine, but also the same type of fluorophores with different substituents should be individually synthesized. Thus, we have designed a diversity-oriented strategy, that is based on continuous Pd-catalyzed cross-coupling reactions, using

fluorescein as the starting material for the efficient synthesis of a series of asymmetric and reduced xanthenes fluorophores (Figure 2D).

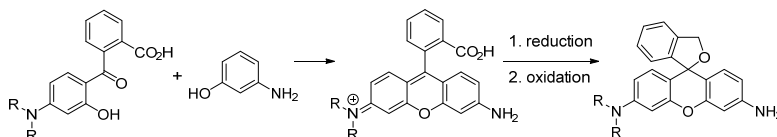
A. Reported synthetic method for asymmetric & reduced fluorescein fluorophore [10,11,23]



B. Reported synthetic method for asymmetric & reduced rhodol fluorophore [9]



C. Reported synthetic method for asymmetric & reduced rhodamine fluorophore [14]



D. This work for diversity-oriented synthesis of asymmetric & reduced fluorophores

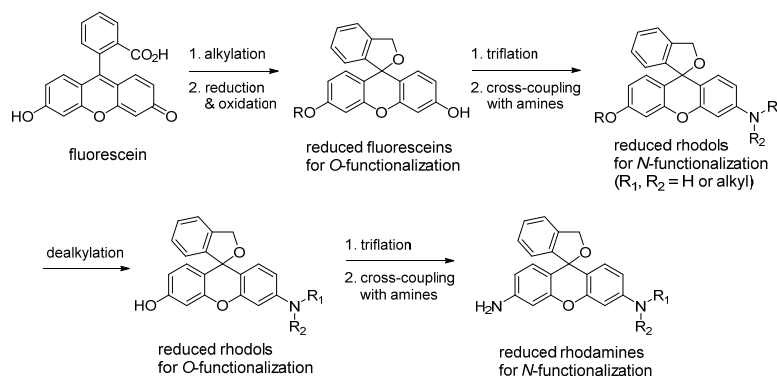


Figure 2. Strategies for synthesizing asymmetric and reduced xanthenes fluorophores.

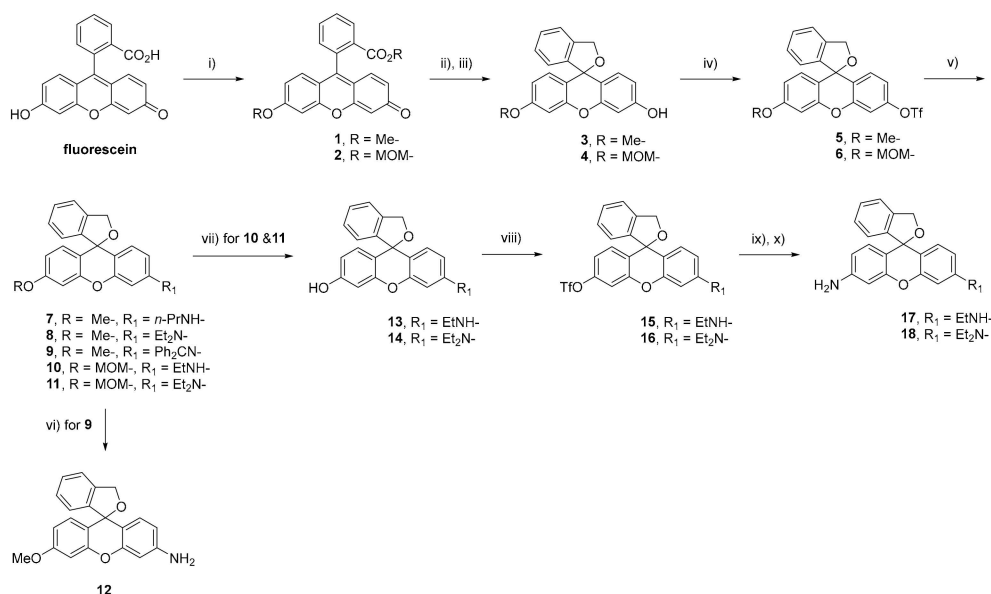
Herein, we describe the synthesis and photochemical properties of a series of asymmetric and reduced xanthenes fluorophores with fluorescein, rhodol, and rhodamine scaffolds, that enable efficient asymmetric *N*-functionalization or *O*-functionalization. Nitroreductase (NTR)-responsive fluorescent probes were developed as activatable fluorescent probes using the various reduced xanthenes fluorophores, which can be applied to the design of new pro-drugs for therapeutics and imaging agents targeting hypoxia [6,23].

2. Results and Discussion

2.1. Chemistry

We started the synthesis of a series of asymmetric and reduced xanthenes fluorophores from commercially available fluorescein, in order to produce fluorophores with synthetic advantage in *O*- and *N*-functionalization of the xanthenes ring, and can be applied as an activatable fluorescent probes. The asymmetric and reduced fluorescein derivative (**3**) for *O*-functionalization was first prepared from fluorescein via dimethylation, LiAlH₄ reduction, and subsequent oxidation with *p*-chloranil (Scheme 1) [10]. We attempted to extend our synthetic strategy to various reduced rhodafuors, including rhodol and rhodamine fluorophores, starting from **3**. Asymmetric and reduced rhodol

derivatives with a monoalkylamino (*n*-propylamino, **7**), dialkylamino (diethylamino, **8**), or free amino (-NH₂, **12**) group were synthesized from **3** via triflation and subsequent Pd-catalyzed cross-coupling reaction, which was developed by Tao Peng et al. [24–27].



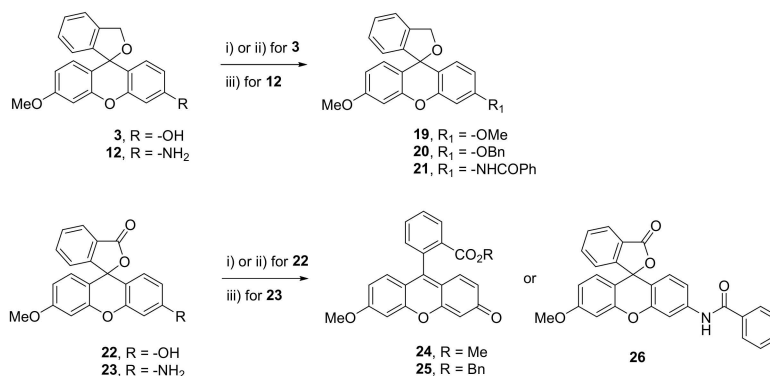
Scheme 1. Synthesis of reduced fluorescein, rhodol, and rhodamine fluorophores. Reagents and conditions: i) CH₃I or methoxymethyl (MOM)-Cl, K₂CO₃. DMF, rt, **1** = 99%, **2** = 89%; ii) LiAlH₄, THF, 0 °C; iii) *p*-chloranil, MeOH, rt, **3** = 79% over 2 steps, **4** = 88% over 2 steps; iv) Tf₂O, pyridine, CH₂Cl₂, 0 °C, to rt, **5** = 86%, **6** = 86%; v) amine or imine, Pd catalyst (Pd(OAc)₂, Pd₂(dba)₃·CHCl₃ or Pd(PPh₃)₄), ligand (BINAP or Xantphos), Cs₂CO₃, toluene, 105 °C, **7** = 20%, **8** = 41%, **9** = further reaction without purification, **10** = 100%, **11** = 47%; vi) aq. 1 N HCl, THF, rt, **12** = 55% over 2 steps; vii) TFA, CH₂Cl₂, rt, **13** = 55%, **14** = 84%; viii) *N*-phenyl-bis-(trifluoromethanesulfonimide), K₂CO₃, CH₃CN, 0 °C, to rt, **15** = 69%, **16** = 57%; ix) benzophenone imine, Pd(OAc)₂, Cs₂CO₃, BINAP, toluene, 105 °C; x) aq. 1 N HCl, THF, rt, **17** = 44% over 2 steps, **18** = 30% over 2 steps.

The cross-coupling reaction, that has been used to prepare the reduced rhodol fluorophores was optimized by the reaction of triflate **5** with diethylamine, in the presence of conventional palladium catalysts (Pd(PPh₃)₄, Pd(OAc)₂, and Pd₂(dba)₃·CHCl₃), ligands (BINAP, Johnphos, and Xantphos), and base (Cs₂CO₃ and *t*-BuONa, data not shown). The use of Pd(OAc)₂ (10 mol%), BINAP (16 mol%), and Cs₂CO₃ (3 eq.) in toluene at 105 °C led to the formation of reduced rhodol derivative **8** bearing a diethylamino group in moderate yield (41%). Under the same condition for the synthesis of **8**, cross-coupling reactions of **5** with *n*-propylamine and benzophenone imine produced reduced rhodol **7**, with an *n*-propylamino group in 20% yield and fluorophore **9**, which was further hydrolyzed, using 1 N HCl in THF to give reduced rhodol derivative **12** with an -NH₂ group (55% yield over 2 steps). The reactions for reduced rhodol **7** and **8** required an excess of *n*-propylamine (20 eq.) and diethylamine (10 eq.), due to their low boiling points, which resulted in relatively low yields.

Next, we attempted to synthesize reduced rhodol **13** and **14** with a -OH group, which are key intermediates for the reduced rhodamine **17** and **18** with an -NH₂ group. We designed a synthetic route, using intermediate **4**, bearing a methoxymethyl (MOM)-protected hydroxyl group, instead of the methoxy group (Scheme 1). Triflate **6** was synthesized in the same manner as **5**, except that the first methylation was replaced by MOM protection using MOMCl. Based on the cross-coupling reaction of **5**, Pd(OAc)₂ and BINAP were used to synthesize the *O*-MOM protected rhodol fluorophores, containing an ethylamino (**10**) and diethylamino (**11**) group, but the reactions were unsuccessful. Thus, the Pd-catalyzed cross-coupling reaction of **6** for reduced rhodols (**10** and **11**) was optimized using a variety of Pd catalysts (Pd(OAc)₂, Pd(PPh₃)₄, Pd(dppf)Cl₂, and Pd₂(dba)₃·CHCl₃)

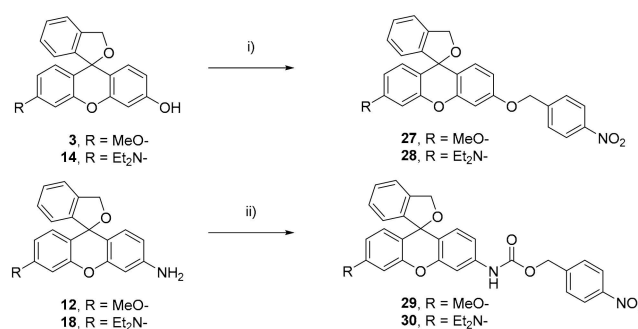
and ligands (BINAP, Xantphos, and Johnphos) (data not shown). Thus, **10** was synthesized in good yield (quant.) under the reaction conditions with Pd₂(dba)₃·CHCl₃ (10 mol%), Xantphos (15 mol%), and Cs₂CO₃ (3 eq.) in toluene at 105 °C, while **11** was prepared in a moderate yield (47%) by using Pd(PPh₃)₄ (10 mol%), BINAP (15 mol%) and Cs₂CO₃ (3 eq.). *O*-MOM protected rhodol derivatives (**10** and **11**) were treated with trifluoroacetic acid to give rhodol fluorophores **13** and **14** bearing a phenolic -OH group for *O*-functionalization. Subsequently, we tried to synthesize reduced rhodamine fluorophores for *N*-functionalization. Triflation of rhodol derivative **13**, using triflic anhydride, gave the desired triflate **15** in very low yield. However, triflation by phenyl triflimide [*N*-phenyl-bis(trifluoromethanesulfonylimide)] and K₂CO₃ in acetonitrile afforded the desired rhodol triflates **15** and **16** in moderate yields (69%, and 57%, respectively). We then performed Pd-catalyzed cross-coupling reactions of **15** and **16** to prepare reduced rhodamine fluorophores possessing an -NH₂ group for *N*-functionalization. The cross-coupling reaction of **15** and **16** with benzophenone imine, using Pd(OAc)₂, BINAP, and Cs₂CO₃ in toluene, followed by acidic hydrolysis produced the desired rhodamine fluorophores **17** and **18** in 44%, and 30% yields, respectively. Previously, various attempts were made for the synthesis of reduced xanthene fluorophores, which resulted in the synthesis of various fluorescein, rhodol, and rhodamine fluorophores from more than one synthetic scheme [9–11,14,23]. The continuous Pd-catalyzed cross-coupling reactions enabled the rapid synthesis of novel series of reduced fluorescein, rhodol, and rhodamine fluorophores in highly efficient and concise synthetic scheme. The library of chemically-stable reduced fluorescein, rhodols, and rhodamines could be constructed with this synthetic strategy in moderate- to high-yields. It can be applied to synthesize various reduced xanthene-based fluorophores with *N*-functionalization or *O*-functionalization, which are useful to the design and discovery of novel activity-based fluorescent probes.

Next, we investigated the reactivity of the reduced xanthene fluorophores in comparison with typical xanthene fluorophores for the *O*-alkylation and amide coupling reactions. We performed *O*-alkylation of reduced fluorescein **3** and typical fluorescein **22**, using methyl iodide and benzyl bromide, under basic conditions (Scheme 2). Both methylation and benzylation of **3** produced the desired *O*-alkylated product in high yields (86%, and 98%, respectively), whereas **22** only gave undesired ester products, which could not be used as activatable fluorescent probes. But the amide coupling reactions of two types of rhodol fluorophores (reduced rhodol **12** and typical rhodol **23**) were different from the *O*-alkylation reactions of **3** and **22**. In the amide coupling reactions, both **12** and **23** afforded the desired amide products (**21**, and **26**, respectively). However, under the reaction conditions, using HOBT and *i*PrNEt₂ in DMF, EDC-coupling of **12** exhibited a six-fold higher yield (50%) than **23** (8%). From the results of alkylation and amide coupling of the two types of xanthene fluorophores, we concluded that reduced xanthene fluorophores are more beneficial for phenolic *O*-alkylation and terminal *N*-amide coupling, compared to typical xanthene fluorophores.



Scheme 2. Reactivity of reduced fluorescein and typical fluorescein fluorophores on alkylation and amide coupling reactions. Reagents and conditions: i) CH₃I, K₂CO₃, DMF, rt, 86% for **19**, 87% for **24**; ii) benzyl bromide, DBU, acetone, rt, 98% for **20**, 71% for **25**; iii) EDC, HOBT, *i*PrNEt₂, DMF, rt, 50% for **21**, 8% for **26**.

We further attempted to synthesize activatable fluorescent probes based on the reduced xanthene fluorophores for sensing nitroreductase, an enzyme that catalyzes the reduction of a nitro group to an amine via a hydroxyl amine in the presence of NADH and a representative biomarker of hypoxic cells including solid tumors [28,29] (Scheme 3). We envisioned that the reduced fluorescein (**3**), rhodol (**12** and **14**), and rhodamine (**18**) fluorophores will be potential candidates for activatable fluorescent probes, because they have a free -OH or NH₂ group and show strong fluorescence at physiological pH (pH~7). The only exception is **12**, which shows weak fluorescence emission at pH~7, but we prepared an activatable fluorescent probe, based on **12** because the concentration of fluorophores released from activatable fluorescent probes can be calculated by the concentration-dependent calibration curve of the corresponding fluorophore. *O*-Alkylated NTR-responsive fluorescent probes (**27** and **28**), based on reduced fluorescein **2** and rhodol **14** containing an -OH group were synthesized using Ag₂O in toluene, according to a previously reported method [6]. Reduced rhodol and rhodamine-based NTR-responsive fluorescent probes (**29** and **30**), bearing a carbamate linker, were prepared from reduced xanthene fluorophores **12** and **18** containing an -NH₂ group, respectively, by using 4-nitrobenzyl chloroformate and *i*PrNEt₂.



Scheme 3. Synthesis of NTR-responsive fluorescent probes with *p*-nitrobenzyl group. Reagents and conditions: i) 4-nitrobenzyl bromide, Ag₂O, toluene, reflux, **27** = 54%, **28** = 48%; ii) 4-nitrobenzyl chloroformate, *i*PrNEt₂, CH₂Cl₂, rt, **29** = 86%, **30** = 47%.

2.2. Photochemical Properties and NTR Reaction

The photochemical properties of the asymmetric and reduced xanthene fluorophores, including quantum yield, concentration-dependent fluorescence emission, stability, and solvent effect, were evaluated. The quantum yields of newly synthesized fluorophores were calculated in comparison with the reference standard, fluorescein (0.1 N NaOH, $\Phi_r = 0.85$; Table 1). Most of reduced xanthene fluorophores exhibited significant quantum yields proving their promising fluorogenic nature. Reduced fluorophores with a -OH showed high quantum yield compared to fluorophore with an -NH₂. Among all fluorophores, rhodol (**13**) and rhodamine (**17**) bearing monoethylamine showed highest quantum yields of 0.824, and 0.399 respectively, showing their strong fluorogenic nature.

Table 1. Quantum Yields of Synthesized Reduced Xanthene Fluorophores.

Comp.	3	7	8	12	13	14	17	18
λ_{abs}	456	473	490	467	472	510	490	504
λ_{em}	518	535	554	519	532	553	537	556
Φ_s^a	0.044	0.010	0.004 ^b	0.013	0.824 ^b	0.141 ^b	0.399	0.042 ^a

a = Quantum yields are measured in water by relative method in comparison with fluorescein (0.1 N NaOH, $\Phi_r = 0.85$), b = reported quantum yields [9,10,14].

Next, the fluorescent emission at the maximal absorption wavelength (λ_{max}) for the asymmetric and reduced xanthene fluorophores in PBS (phosphate buffered saline; 10 mM, pH 7.4) was evaluated in a concentration-dependent manner (Figure 3). The reduced fluorescein (**3**), rhodol (**13** and **14**),

and rhodamine (**17** and **18**), containing a -OH or -NH₂ group, showed very strong fluorescence emission at physiological pH~7.4, whereas reduced rhodol **7** and **8**, without the -OH or -NH₂ group, showed relatively weak fluorescence emission at pH~7.4. Reduced rhodol **8** with a -OCH₃ and -NEt₂ groups exhibited extremely low fluorescence and quantum yield, implying that an acidic hydrogen on the terminal oxygen or nitrogen atom on the xantheno ring is essential for sufficiently intense fluorescence emission in this series of fluorophores. The rhodol **12** showed exceptionally low fluorescent emission (about 2000 RFU at 5 μM) in the series, even though it contains an -NH₂ group. Of all the reduced xantheno fluorophores containing the novel rhodol (**7**, **8** and **12**) and rhodamine (**17**) derivatives, the rhodamine **17** containing -NH₂ and -NH₂ groups showed the strongest fluorescence emission (about 80,000 RFU at 2 μM; Figure 3G).

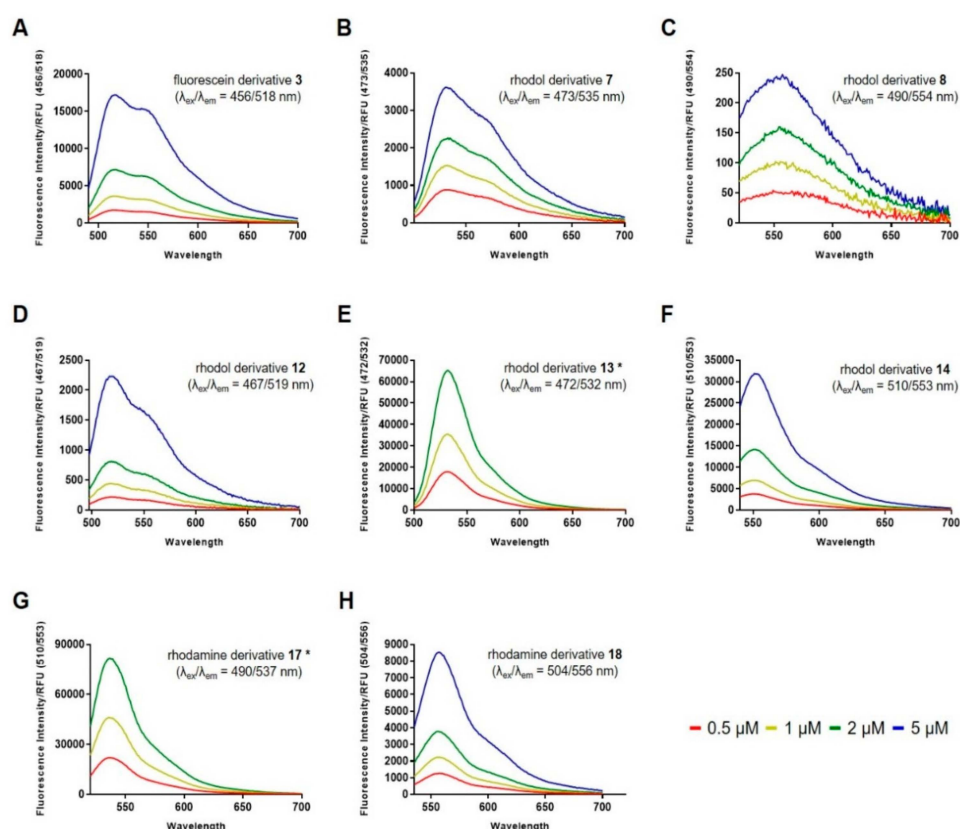


Figure 3. Concentration-dependent fluorescence spectra of asymmetric and reduced xantheno fluorophores in PBS (10 mM, pH 7.4). (A) fluorescein **3** ($\lambda_{ex}/\lambda_{em} = 456/518$ nm); (B) rhodol **7** ($\lambda_{ex}/\lambda_{em} = 473/535$ nm); (C) rhodol **8** ($\lambda_{ex}/\lambda_{em} = 490/554$ nm); (D) rhodol **12** ($\lambda_{ex}/\lambda_{em} = 467/519$ nm); (E) rhodol **13** ($\lambda_{ex}/\lambda_{em} = 472/532$ nm); (F) rhodol **14** ($\lambda_{ex}/\lambda_{em} = 510/553$ nm); (G) rhodamine **17** ($\lambda_{ex}/\lambda_{em} = 490/537$ nm); (H) rhodamine **18** ($\lambda_{ex}/\lambda_{em} = 504/556$ nm). *Fluorescence of rhodol (**13**) and rhodamine (**17**) derivatives with monoethylamino group was estimated in the range 0.5 to 2 μM because fluorescence at 5 μM is over threshold.

However, the pH-dependent fluorescence spectra showed a different trend from physiological pH (Figure 4). Reduced rhodol fluorophores (**13** and **14**) showed strong fluorescence in the pH range of 5–11, indicating that it is feasible to apply them to activatable fluorescent probes for use under physiological conditions, as demonstrated previously [11,12]. On the other hand, the reduced fluorescein (**3**) and rhodamine (**17** and **18**) fluorophores exhibited, not only strong fluorescence at physiological pH, but also significantly enhanced fluorescence emission upon lowering the pH. Interestingly, reduced rhodol **7** and **12**, containing a -OCH₃ at the end and mono-substituted amine (-NHPr), or free amine (-NH₂), at the other end exhibited very weak fluorescence at physiological pH 7.4, but showed a significant increase in fluorescence below pH 6.

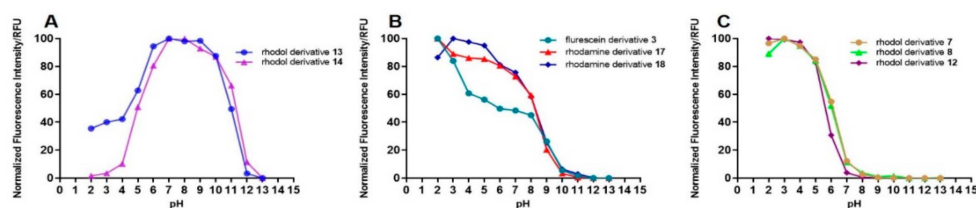


Figure 4. pH-Dependent fluorescence spectra of asymmetric and reduced xanthene fluorophores (Normalized fluorescence intensity plotted against pH at 1.0 μM) in buffers with pH ranging from 2 to 13. (A) rhodol **13** ($\lambda_{\text{ex}}/\lambda_{\text{em}} = 472/532$ nm) and rhodol **14** ($\lambda_{\text{ex}}/\lambda_{\text{em}} = 510/553$ nm); (B) fluorescein **3** ($\lambda_{\text{ex}}/\lambda_{\text{em}} = 456/518$ nm), rhodamine **17** ($\lambda_{\text{ex}}/\lambda_{\text{em}} = 490/537$ nm) and rhodamine **18** ($\lambda_{\text{ex}}/\lambda_{\text{em}} = 504/556$ nm); (C) rhodol **7** ($\lambda_{\text{ex}}/\lambda_{\text{em}} = 473/535$ nm), rhodol **8** ($\lambda_{\text{ex}}/\lambda_{\text{em}} = 490/554$ nm) and rhodol **12** ($\lambda_{\text{ex}}/\lambda_{\text{em}} = 467/519$ nm)..

We then investigated the solvent effect on the fluorescence emission of the asymmetric and reduced xanthene fluorophores (Figure 5). It is well known that the fluorescence of xanthene dyes is complicated by the presence of a solvent-dependent equilibrium, between the colored open form bearing a zwitterion, and the colorless closed lactone form in protic solvents [30–32]. Urano’s group reported a series of reduced rhodol and rhodamine fluorophores, and concluded that the lifetime of the open form of reduced xanthene dyes is very important in determining fluorescence emission [11]. In addition to their results, we envisioned that the nucleophilicity of the benzylic alkoxide will shift the equilibrium towards non-fluorescent closed form, as the spirocyclization of the open form is induced by the nucleophilic addition of benzyl alkoxide (Figure 1B). As observed in many $\text{S}_{\text{N}}2$ and nucleophilic addition reactions, polar protic solvents, such as water and methanol, can stabilize the nucleophile via solvation by hydrogen bonding and decrease its reactivity, whereas polar aprotic solvents, such as DMSO (dimethyl sulfoxide), which has a strong dipole moment, but cannot form H-bonds, enhance the reactivity of the nucleophile. Thus, we investigated the solvent effect on the fluorescence emission of reduced xanthene dyes, in order to evaluate the nucleophilicity of benzyl alkoxide in equilibrium between the closed and open forms (Figure 5). We measured the fluorescence emission of our reduced xanthene fluorophores (1.0 μM) in various solvents, including water ($\epsilon_{\text{r}} = 78.5$ at 25 $^{\circ}\text{C}$), methanol ($\epsilon_{\text{r}} = 32.6$ at 25 $^{\circ}\text{C}$), ethanol ($\epsilon_{\text{r}} = 24.6$ at 25 $^{\circ}\text{C}$), isopropanol (IPA, $\epsilon_{\text{r}} = 18.3$ at 25 $^{\circ}\text{C}$), and DMSO ($\epsilon_{\text{r}} = 47.0$ at 25 $^{\circ}\text{C}$). Most of the reduced xanthene dyes showed the strongest fluorescence in water and the weakest fluorescence in DMSO. The trends in the fluorescence emission, observed in polar protic solvents, were proportional to the dipole moment of the solvent, except for reduced rhodol fluorophore **14**. The fluorescence emission in polar protic solvents decreased with the decreasing dipole moment of the solvent. Whereas, a polar aprotic solvent DMSO, with a dielectric constant between those of water and methanol, showed lesser fluorescence emission, compared to the polar protic solvent for all the reduced xanthene fluorophores. The solvent effect on fluorescence emission implies that the nucleophilicity of benzyl alkoxide in the reduced xanthene fluorophores affects the equilibrium between the fluorescent open form and non-fluorescent closed form. However, the structure-based fluorescence emission of xanthene dyes in equilibrium is very complicated; for example, xanthene dyes exist in several neutral and ionic forms in solution and their equilibria is susceptible to a variety of factors, including concentration, pH, temperature, and solvent, etc. [30,31,33–36].

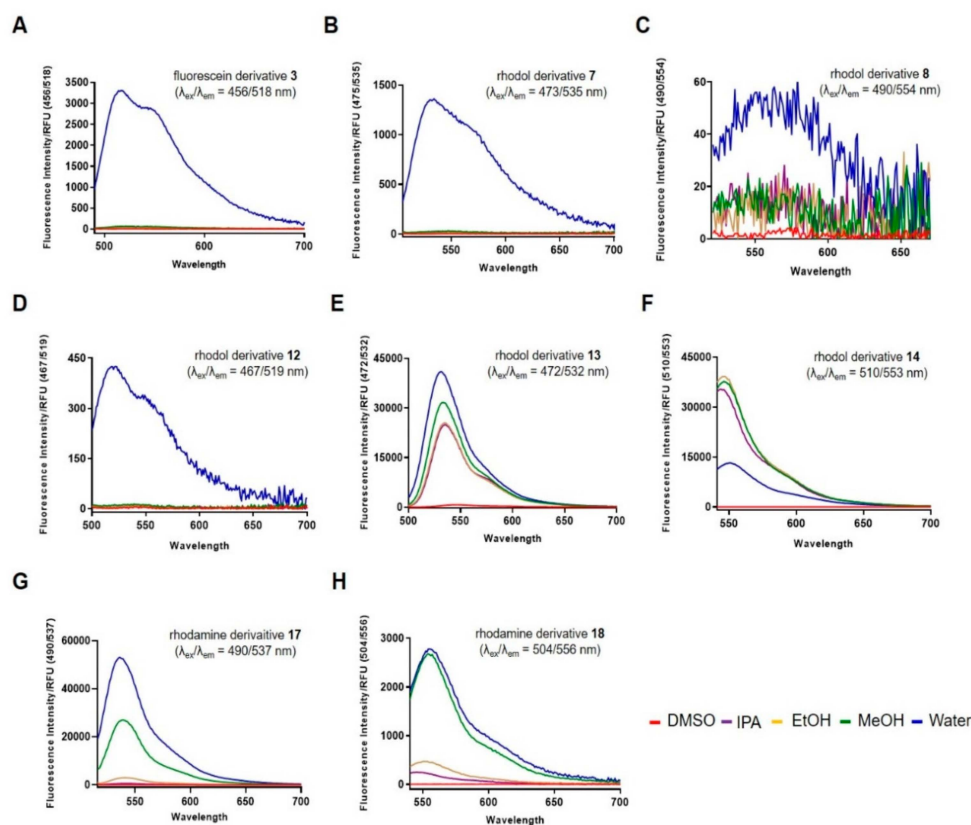


Figure 5. Solvent effect of asymmetric and reduced xanthene fluorophores (1.0 μM) in DMSO, IPA, EtOH, MeOH, and water. (A) fluorescein 3 ($\lambda_{\text{ex}}/\lambda_{\text{em}} = 456/518$ nm); (B) rhodol 7 ($\lambda_{\text{ex}}/\lambda_{\text{em}} = 473/535$ nm); (C) rhodol 8 ($\lambda_{\text{ex}}/\lambda_{\text{em}} = 490/554$ nm); (D) rhodol 12 ($\lambda_{\text{ex}}/\lambda_{\text{em}} = 467/519$ nm); (E) rhodol 13 ($\lambda_{\text{ex}}/\lambda_{\text{em}} = 472/532$ nm); (F) rhodol 14 ($\lambda_{\text{ex}}/\lambda_{\text{em}} = 510/553$ nm); (G) rhodamine 17 ($\lambda_{\text{ex}}/\lambda_{\text{em}} = 490/537$ nm); (H) rhodamine 18 ($\lambda_{\text{ex}}/\lambda_{\text{em}} = 504/556$ nm).

Finally, we applied our asymmetric and reduced xanthene fluorophores as activatable fluorescent probes targeting nitroreductase. We chose four representative fluorophores, including fluorescein 3, rhodols 12 and 14, and rhodamine 18, to develop NTR-responsive fluorescent probes. Reduced rhodol 12 showed weaker fluorescence as compared to the other fluorophores, employed as NTR-responsive probes. Nevertheless, we chose 12 as a fluorophore for activatable fluorescent probe, as the concentration-dependent fluorescence calibration curve could be established, so that the concentration of the fluorophore, released from the NTR-responsive fluorescent probe, could be determined. As reported in our previous work on NTR-responsive fluorescent probes [6], xanthene fluorophores are linked to the *p*-nitrobenzyl group via an ether (27 and 28) or carbamate (29 and 30) moiety, and reduction of the nitro group in the probe triggers the release of the fluorophore via 1,6-rearrangement elimination of the *p*-aminobenzyl group, leading to a turn-on fluorescent response.

The stability of the linkage in the NTR-responsive fluorescent probes (27–30) was assessed by estimating the fluorescence emission under varying temperature and pH conditions (Figure 6). All the probes showed weak, but stable, fluorescence emissions in the temperature range 25 to 45 $^{\circ}\text{C}$ and pH range 5–13, implying that they can be applied as activatable fluorescent probes for sensing a specific protein, NTR, under physiological conditions. Exceptionally, the strong fluorescence emission of reduced rhodamine-based probe 30, containing a carbamate linkage, present in acidic pH range between 2 to 4, is the result of the fluorophore via hydrolysis under acidic conditions, which is highly correlated with the pH-dependent fluorescence spectrum of fluorophore 18 (Figure 4H).

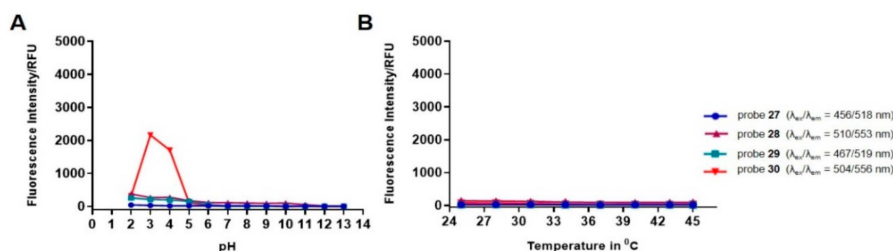


Figure 6. Stability of nitroreductase (NTR)-responsive fluorescent probes (1.0 μM). (A) Effect of variation in pH from 2 to 13 at 25 $^{\circ}\text{C}$; (B) Effect of variation in temperature (25, 28, 31, 34, 37, 43, and 45 $^{\circ}\text{C}$) in PBS (10 mM, pH 7.4).

We performed kinetic studies (1.0 μM of probes) of probes during the NTR reaction, using 10 $\mu\text{g}/\text{mL}$ of this protein as a function of time, in order to investigate the activatable response of probes to NTR (Figure 7). Probe 27 and 28, which are fluorescein- and rhodol-based activatable fluorescent probes, containing an ether linkage, showed strong fluorescence responses over time in the presence of NTR (Figure 7A). On the other hand, probes 29 and 30, bearing a carbamate linkage, which were prepared via *N*-functionalization of the reduced rhodol and rhodamine fluorophores containing an $-\text{NH}_2$ group, showed relatively weak fluorescence emission over time during the NTR reaction.

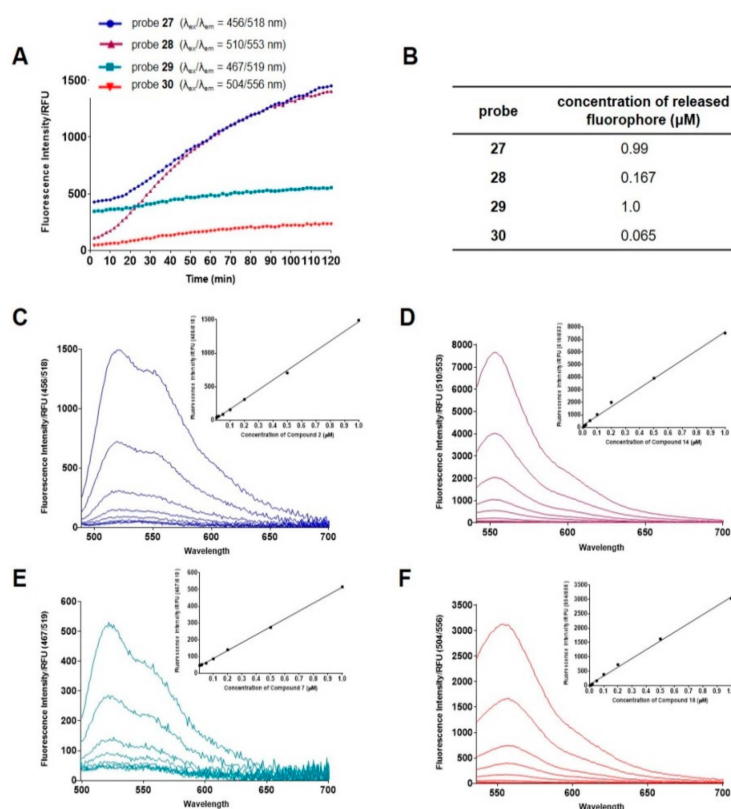


Figure 7. Kinetic study of NTR-responsive fluorescent probes and fluorescence calibration curves of corresponding fluorophores. (A) Plot of fluorescence emission of probes (1.0 μM) with reaction time in the presence of 10 $\mu\text{g}/\text{mL}$ of NTR, NADH (500 μM), PBS (pH 7.4), and incubation at 37 $^{\circ}\text{C}$; (B) Calculated concentrations of the corresponding fluorophores released from NTR-responsive fluorescent probes during NTR reaction; (C–F) Calibration curves at concentrations of 0.005, 0.01, 0.02, 0.05, 0.1, 0.2, 0.5, and 1.0 μM of fluorophore (Inset: Linear regression graph); Concentration-dependent changes in the fluorescence emission of fluorophore 3 (C), 14 (D), 12 (E), and 18 (F).

We determined the concentration of the released fluorophores in the NTR reaction using the concentration-dependent calibration curves obtained for the fluorophores (Figure 7B–F). Distinctly

different results were obtained from the calibration curves: Probes **27** and **29** showed the completion of the NTR reaction with almost 1.0 μM of the released fluorophore (**3** and **12**), whereas the concentration of the fluorophore released from probes **28** and **30**, reached only 0.167 μM (**14**) and 0.065 μM (**18**) (Figure 7B). Although, probe **29** gave 100% yield for the NTR reaction, the corresponding fluorophore **12** could not be applied as an activatable imaging probe at physiological pH due to its photochemical nature, i.e., weak fluorescence emission at physiological pH. Rhodamine-based fluorophore **18** showed enough fluorescence at physiological pH, but the corresponding NTR-responsive fluorescent probe **30** exhibited a poor release of the fluorophore, during the NTR reaction, demonstrating that **18** is not a good candidate for an activatable fluorescent probe. The reduced fluorescein **3** and rhodol **14** fluorophores, bearing an -OH group showed strong fluorescence at physiological pH, and the corresponding NTR-responsive fluorescent probes (**27** and **28**), also emitted strong fluorescence during the NTR reaction. However, probe **28**, based on the reduced rhodol gave a relatively low yield (~17%) in the NTR reaction, as compared to probe **27**. Taken together, the NTR reaction revealed that **3** and **14** are promising candidates for activatable fluorescent probes, and among all the asymmetric and reduced fluorophores studied, fluorescein **3** is the best choice for an activatable fluorescent probe.

3. Materials and Methods

3.1. Materials and Instrumentation

All reagents and solvents were purchased from Sigma-Aldrich Chemical Co. (St. Louis, USA), Tokyo Chemical Industries (Tokyo, Japan), Daejung Chemicals (Siheung-si, Korea), and Alfa Aesar (Ward Hill, MA, USA) and used without any further purification. Anhydrous solvents were purchased from Sigma-Aldrich Chemical Co. (St. Louis, MO, USA), and all reactions were performed under nitrogen atmosphere. Silica gel (ZEOprep 60 40–63 μm , Zeochem, Louisville, KY, USA) was used for flash column chromatography, and silica gel plates (Kiesegel 60F₂₅₄, Merck, Darmstadt, Germany) were used for thin-layer chromatography. ¹H and ¹³C-NMR spectra were measured on a JEOL JNM-ECZ400s/L1 (400 MHz) spectrometer (Jeol, Tokyo, Japan), with CDCl₃ or DMSO-*d*₆ as the NMR solvent (Cambridge Isotope Laboratories, Tewksbury, MA, USA). Chemical shifts are expressed in parts per million (ppm), and the coupling constant *J* is reported in hertz (Hz). Chemical shifts (in ppm) in ¹H-NMR are based on the chemical shift of tetramethylsilane ($\delta = 0$ ppm) in CDCl₃ as an internal standard. The chemical shifts in ¹³C-NMR are reported in ppm relative to the centerline of the triplet at 77.0 ppm observed for CDCl₃ or 39.5 ppm for DMSO-*d*₆. All in vitro enzyme assays were performed by recording the absorbance and emission using a Synergy™ H1 microplate reader from BioTek Instruments (Winooski, VT, USA). Nitroreductase from *Escherichia coli* and NADH were purchased from Sigma-Aldrich Chemical Co. The lyophilized nitroreductase powder was dissolved in deionized water, fractionated, and immediately stored at -80 °C.

3.2. General Synthetic Procedures

3.2.1. General Procedure A: Alkylation

K₂CO₃ (2.5 eq.) was added to a solution of fluorescein (1.0 eq.) in DMF, and the reaction mixture stirred at rt for 1 h under N₂ atmosphere. Methyl iodide or chloromethyl methyl ether (3.0 eq.) was added dropwise to the reaction mixture, using a syringe pump with the rate of 5 mL/1hr, and the reaction mixture stirred at rt for 3–12 h. After completion of the reaction, ice water was added to the reaction mixture and stirred at 0 °C for 30 min. The resulting yellow solid was filtered (in the case of the MOM protection reaction, extraction was performed using ethyl acetate) and washed with water to completely remove K₂CO₃. The resulting solid was dried or purified by column chromatography to afford the desired compound.

3.2.2. General Procedure B: LiAlH₄ Reduction and p-Chloranil Oxidation

To a solution of compound **1** or **2** (1.0 eq.) in anhydrous THF was added LiAlH₄ (2.0 eq.) at 0 °C. The reaction mixture was stirred at 0 °C for 4 h. After completion of the reaction, sodium sulfate decahydrate (5.6 eq.) was added to the reaction mixture at 0 °C and then stirred at rt for 30 min. The reaction mixture was filtered through a short pad of Celite, which was washed with CH₂Cl₂. The filtrate was concentrated in vacuo, and the crude product used in the next reaction without further purification. The crude compound, obtained from the LiAlH₄ reduction, was dissolved in MeOH, followed by the addition of p-chloranil (3.0 eq.), and stirred at rt for 2 h. The reaction mixture was filtered, and the filtrate concentrated in vacuo. The residue was purified by flash column chromatography on silica gel to give the desired product.

3.2.3. General Procedure C: Triflation

To a solution of the phenol derivative (1.0 eq.) in anhydrous CH₂Cl₂ or CH₃CN was added pyridine, or K₂CO₃ (4.0 eq.), respectively, and the reaction mixture stirred at 0 °C for 20 min. Triflic anhydride or N-phenyl-bis(trifluoromethanesulfonylimide) (2.0 eq.) was slowly added to the reaction mixture over 30 min, and then, the mixture was allowed to warm to rt and stirred for 3 h. The reaction was quenched with water and extracted with CH₂Cl₂. The organic layer was washed with aqueous 1 N HCl solution or saturated NH₄Cl aqueous solution, followed by water and brine. The organic layer was dried over Na₂SO₄, filtered and concentrated in vacuo. The residue was purified by flash column chromatography on silica gel to give the desired product.

3.2.4. General Procedure D: Pd-Catalyzed Cross Coupling Reaction

All glassware was dried in an oven before use. To a solution of the corresponding triflate (1.0 eq.) and amine (10 or 20 eq.) or benzophenone imine (1.2 eq.) in anhydrous toluene were added Pd(OAc)₂, Pd(PPh₃)₄, or Pd₂(dba)₃.CHCl₃ (0.1 eq.), BINAP or Xantphos (0.16 eq.), and Cs₂CO₃ (3.0 eq.), and the reaction mixture was heated at 105 °C for 4–12 h under N₂ atmosphere. After completion of the reaction, the mixture was filtered through a short pad of Celite and washed with CH₂Cl₂. The filtrate was concentrated in vacuo, and the residue was purified by flash column chromatography on silica gel to give the desired product.

3.2.5. General Procedure E: MOM-Deprotection

To a solution of the corresponding MOM protected compound (100 mg) in anhydrous CH₂Cl₂ (1 mL) at 0 °C, a solution of trifluoroacetic acid in CH₂Cl₂ [1 mL, TFA:CH₂Cl₂ = 1:1 (v/v)] was slowly added dropwise at 0 °C. After the addition of TFA was complete, the reaction mixture was allowed to warm to rt and stirred at rt for 1 h. The reaction was quenched with 1 N NaOH solution and extracted with CH₂Cl₂. The organic layer was dried over Na₂SO₄, filtered, and concentrated in vacuo. The residue was purified by flash column chromatography on silica gel to give the desired product.

3.3. Determination of Fluorescence Quantum Yield

The quantum yield (Φ_s) of the newly synthesized reduced xanthene fluorophores was determined by comparing the integrated area under the curve of the sample, excited at 490 nm, with the reference fluorophore. Fluorescein ($\Phi_r = 0.85$, 0.1 N NaOH) is used as the reference fluorophore for determining the quantum yield of reduced xanthene fluorophore. Absorption spectra and fluorescence spectra of fluorophores were recorded on Synergy H1TM microplate reader (BioTek Instruments, Winooski, VT, USA) and FluoroMate FS-2 fluorescence spectrometer (Scinco, Seoul, Korea), respectively. The absorbance values are kept below 0.1 in order to minimize re-absorption effects. Fluorescence quantum yield (Φ_s) of reduced xanthene fluorophores was calculated by using following Equation (1):

$$\Phi_s = \Phi_r \times \left(\frac{A_r}{A_s}\right) \times \left(\frac{F_s}{F_r}\right) \times \left(\frac{\eta_s}{\eta_r}\right)^2 \quad (1)$$

Φ_s = Quantum yield of sample; A_r = Absorbance of reference at excitation wavelength; A_s = Absorbance of sample at excitation wavelength; F_r = Integrated area under emission curve of reference; F_s = Integrated area under emission curve of sample; η_r = Refractive index of solvent of reference; η_s = Refractive index of solvent of sample; and Φ_r = Quantum yield of fluorescein.

3.4. Concentration-Dependent Fluorescence Study of Fluorophores

A concentration-dependent study was performed by incubating different concentration, such as 0.5, 1, 2, and 5 μM of the fluorophore in PBS (pH 7.4) at 25 $^\circ\text{C}$, and recording the fluorescence spectra at each concentration in 96-well microplate using Synergy H1 reader.

3.5. Effect of pH on Fluorescence Intensity of Fluorophores

A pH-dependent fluorescence change of fluorophore was performed by incubating 1 μM of the probe in a range of pH buffer solutions (pH 2 to 13) at 25 $^\circ\text{C}$, and recording the fluorescence at each pH in 96-well microplate, using SynergyTM H1 (BioTek Instruments).

3.6. Solvent Effect on the Fluorescence Emission of Fluorophores

The effect of solvent polarity on the fluorescent intensity was measured by incubating 1 μM of the fluorophore in different solvents, including water, methanol, ethanol, isopropanol, and DMSO. The fluorescence was measured at the respective excitation wavelength of the fluorophore, in a 96-well microplate, using SynergyTM H1 (BioTek Instruments).

3.7. In vitro Nitroreductase Assay

All spectroscopic readings were recorded on SynergyTM H1 (BioTek Instruments) using a 96-well microplate. The NTR reaction was performed in a total volume of 200 μL with the addition of 100 μL of PBS (10 mM, pH 7.4), 10 μL of probe stock solution (20 μM in DMSO), 20 μL of NADH solution (5 mM in 0.01 M aq. NaOH), and an appropriate volume of NTR solution (10 $\mu\text{g}/100 \mu\text{L}$ in distilled water). The final volume was adjusted to 200 μL using PBS. The plate was incubated at 37 $^\circ\text{C}$ for an appropriate length of time with continuous shaking, and the emission spectra were recorded at the respective wavelengths with respect to time to prepare kinetic graph.

3.8. pH and Thermal Stability of Fluorescent Probes

A temperature-dependent assay was performed by incubating 1 μM of the probe in PBS (pH 7.4) at different temperatures for 20 min, and recording the fluorescence at each temperature. A pH-dependent study was performed by incubating 1 μM of the probe in a range of pH buffer solutions (pH 2 to 13) at 25 $^\circ\text{C}$ and recording the fluorescence at each pH in 96-well microplate, using SynergyTM H1 (BioTek Instruments).

All synthetic procedures, ¹H-NMR, ¹³C-NMR and HRMS of all compounds can be seen in the Supplementary Materials.

4. Conclusions

In conclusion, we developed a highly efficient and versatile synthetic route to a series of asymmetric and reduced xanthene fluorophores, including fluorescein, rhodol, and rhodamine derivatives, which are representative xanthene scaffold-based dyes, and employed them as activatable fluorescent probes for sensing nitroreductase. A variety of asymmetric and reduced xanthene fluorophores, bearing an -OH or -NH₂ group, capable of *O*- or *N*-functionalization to prepare activatable fluorescent probes, were synthesized from commercially available fluorescein by continuous Pd-catalyzed cross-coupling reactions. Their photochemical properties, including quantum yields,

fluorescence emission under various conditions (variation in concentrations, pH, and solvents) were characterized. Two fluorophores, including fluorescein (**3**) and rhodol (**14**) bearing an -OH group for O-functionalization, and two other fluorophores, including rhodol (**12**) and rhodamine (**18**), containing an -NH₂ group for N-functionalization were subjected to develop NTR-responsive fluorescent probes. These probes exhibited turn-on fluorescence by releasing the fluorophore in the NTR reaction. This work demonstrates that the asymmetric and reduced xanthene fluorophores synthesized using our strategy are useful in developing activatable fluorescent probes for diverse biological applications under physiological conditions.

Supplementary Materials: Figures S1–S27: Synthetic procedures, ¹H-NMR, ¹³C-NMR and HRMS of all compounds.

Author Contributions: Conceptualization, D.-J.C.; methodology, T.-H.L. and J.K.; validation, K.N.M and H.Y.; formal analysis, S.-T.Y.; writing original draft preparation, K.N.M. and T.-H.L.; and supervision, D.-J.C.

Funding: This research was supported by the National Research Foundation of Korea (NRF) funded by the Ministry of Science, ICT, and Future Planning (NRF-2016R1C1B1009901, NRF-2018R1D1A1B07050581 & NRF-2019R1F1A1063304).

Conflicts of Interest: The authors declare no competing financial interest.

References

1. Kobayashi, H.; Ogawa, M.; Alford, R.; Choyke, P.L.; Urano, Y. New Strategies for Fluorescent Probe Design in Medical Diagnostic Imaging. *Chem. Rev.* **2010**, *110*, 2620–2640. [[CrossRef](#)] [[PubMed](#)]
2. Beija, M.; Afonso, C.A.M.; Martinho, J.M.G. Synthesis and Applications of Rhodamine Derivatives as Fluorescent Probes. *Chem. Soc. Rev.* **2009**, *38*, 2410–2433. [[CrossRef](#)] [[PubMed](#)]
3. Whitaker, J.E.; Haugland, R.P.; Ryan, D.; Hewitt, P.C.; Haugland, R.P.; Prendergast, F.G. Fluorescent Rhodol Derivatives: Versatile, Photostable Labels and Tracers. *Anal. Biochem.* **1992**, *207*, 267–279. [[CrossRef](#)]
4. Lacivita, E.; Leopoldo, M.; Berardi, F.; Colabufo, N.A.; Perrone, R. Activatable Fluorescent Probes: A New Concept in Optical Molecular Imaging. *Curr. Med. Chem.* **2012**, *19*, 4731–4741. [[CrossRef](#)] [[PubMed](#)]
5. Zhao, J.; Jin, G.; Weng, G.; Li, J.; Zhu, J.; Zhao, J. Recent Advances in Activatable Fluorescence Imaging Probes for Tumor Imaging. *Drug Discov. Today* **2017**, *22*, 1367–1374. [[CrossRef](#)] [[PubMed](#)]
6. More, K.N.; Lim, T.H.; Kim, S.Y.; Kang, J.; Inn, K.S.; Chang, D.J. Characteristics of New Bioreductive Fluorescent Probes Based on the Xanthene Fluorophore: Detection of Nitroreductase and Imaging of Hypoxic Cells. *Dyes Pigm.* **2018**, *151*, 245–253. [[CrossRef](#)]
7. Song, F.; Garner, A.L.; Koide, K. A Highly Sensitive Fluorescent Sensor for Palladium Based on the Allylic Oxidative Insertion Mechanism. *J. Am. Chem. Soc.* **2007**, *129*, 12354–12355. [[CrossRef](#)]
8. Song, F.; Watanabe, S.; Floreancig, P.E.; Koide, K. Oxidation-Resistant Fluorogenic Probe for Mercury Based on Alkyne Oxymercuration. *J. Am. Chem. Soc.* **2008**, *130*, 16460–16461. [[CrossRef](#)]
9. Kamiya, M.; Asanuma, D.; Kuranaga, E.; Takeishi, A.; Sakabe, M.; Miura, M.; Nagano, T.; Urano, Y. β -Galactosidase Fluorescence Probe with Improved Cellular Accumulation Based on a Spirocyclized Rhodol Scaffold. *J. Am. Chem. Soc.* **2011**, *133*, 12960–12963. [[CrossRef](#)]
10. Asanuma, D.; Sakabe, M.; Kamiya, M.; Yamamoto, K.; Hiratake, J.; Ogawa, M.; Kosaka, N.; Choyke, P.L.; Nagano, T.; Kobayashi, H.; et al. Sensitive β -galactosidase-Targeting Fluorescence Probe for Visualizing Small Peritoneal Metastatic Tumours In Vivo. *Nat. Commun.* **2015**, *6*, 6463. [[CrossRef](#)]
11. Uno, S.; Kamiya, M.; Yoshihara, T.; Sugawara, K.; Okabe, K.; Tarhan, M.C.; Fujita, H.; Funatsu, T.; Okada, Y.; Tobita, S.; et al. A Spontaneously Blinking Fluorophore Based on Intramolecular Spirocyclization for Live-Cell Super-Resolution Imaging. *Nat. Chem.* **2014**, *6*, 681–689. [[CrossRef](#)] [[PubMed](#)]
12. Iwatate, R.J.; Kamiya, M.; Urano, Y. Asymmetric Rhodamine-Based Fluorescent Probe for Multicolour In Vivo Imaging. *Chem. Eur. J.* **2016**, *22*, 1696–1703. [[CrossRef](#)] [[PubMed](#)]
13. Au-Yeung, H.Y.; Chan, J.; Chantarojsiri, T.; Chang, C.J. Molecular Imaging of Labile Iron(II) Pools in Living Cells with a Turn-On Fluorescent Probe. *J. Am. Chem. Soc.* **2013**, *135*, 15165–15173. [[CrossRef](#)] [[PubMed](#)]

14. Sakabe, M.; Asanuma, D.; Kamiya, M.; Iwatate, R.J.; Hanaoka, K.; Terai, T.; Nagano, T.; Urano, Y. Rational Design of Highly Sensitive Fluorescence Probes for Protease and Glycosidase Based on Precisely Controlled Spirocyclization. *J. Am. Chem. Soc.* **2013**, *135*, 409–414. [[CrossRef](#)] [[PubMed](#)]
15. Fujii, T.; Kamiya, M.; Urano, Y. In Vivo Imaging of Intraperitoneally Disseminated Tumors in Model Mice by Using Activatable Fluorescent Small-Molecular Probes for Activity of Cathepsins. *Bioconjugate Chem.* **2014**, *25*, 1838–1846. [[CrossRef](#)] [[PubMed](#)]
16. Taki, M.; Akaoka, K.; Mitsui, K.; Yamamoto, Y. A Mitochondria-Targeted Turn-On Fluorescent Probe Based on a Rhodol Platform for the Detection of Copper(I). *Org. Biomol. Chem.* **2014**, *12*, 4999–5005. [[CrossRef](#)]
17. Niwa, M.; Hirayama, T.; Okuda, K.; Nagasawa, H. A New Class of High-Contrast Fe(II) Selective Fluorescent Probes Based on Spirocyclized Scaffolds for Visualization of Intracellular labile Iron Delivered by Transferrin. *Org. Biomol. Chem.* **2014**, *12*, 6590–6597. [[CrossRef](#)]
18. Castelló Beltrán, C.; Palmer, E.A.; Buckley, B.R.; Iza, F. Virtues and Limitations of Pittsburgh Green for Ozone Detection. *Chem. Commun.* **2015**, *51*, 1579–1582. [[CrossRef](#)]
19. Doura, T.; Kamiya, M.; Obata, F.; Yamaguchi, Y.; Hiyama, T.Y.; Matsuda, T.; Fukamizu, A.; Noda, M.; Miura, M.; Urano, Y. Detection of LacZ-Positive Cells in Living Tissue with Single-Cell Resolution. *Angew. Chem. Int. Ed.* **2016**, *55*, 9620–9624. [[CrossRef](#)]
20. Best, Q.A.; Prasai, B.; Rouillere, A.; Johnson, A.E.; McCarley, R.L. Efficacious Fluorescence Turn-On Probe for High-Contrast Imaging of Human Cells Overexpressing Quinone Reductase Activity. *Chem. Commun.* **2017**, *53*, 783–786. [[CrossRef](#)]
21. Yogo, T.; Umezawa, K.; Kamiya, M.; Hino, R.; Urano, Y. Development of an Activatable Fluorescent Probe for Prostate Cancer Imaging. *Bioconjugate Chem.* **2017**, *28*, 2069–2076. [[CrossRef](#)] [[PubMed](#)]
22. Kuriki, Y.; Kamiya, M.; Kubo, H.; Komatsu, T.; Ueno, T.; Tachibana, R.; Hayashi, K.; Hanaoka, K.; Yamashita, S.; Ishizawa, T.; et al. Establishment of Molecular Design Strategy to Obtain Activatable Fluorescent Probes for Carboxypeptidases. *J. Am. Chem. Soc.* **2018**, *140*, 1767–1773. [[CrossRef](#)] [[PubMed](#)]
23. Atwell, G.J.; Yang, S.; Pruijn, F.B.; Pullen, S.M.; Hogg, A.; Patterson, A.V.; Wilson, W.R.; Denny, W.A. Synthesis and Structure–Activity Relationships for 2,4-Dinitrobenzamide-5-mustards as Prodrugs for the Escherichia coli nfsB Nitroreductase in Gene Therapy. *J. Med. Chem.* **2007**, *50*, 1197–1212. [[CrossRef](#)] [[PubMed](#)]
24. Peng, T.; Yang, D. Construction of a Library of Rhodol Fluorophores for Developing New Fluorescent Probes. *Org. Lett.* **2010**, *12*, 496–499. [[CrossRef](#)] [[PubMed](#)]
25. Grimm, J.B.; Lavis, L.D. Synthesis of Rhodamines from Fluoresceins Using Pd-Catalyzed C–N Cross-Coupling. *Org. Lett.* **2011**, *13*, 6354–6357. [[CrossRef](#)]
26. Butkevich, A.N.; Mitronova, G.Y.; Sidenstein, S.C.; Klocke, J.L.; Kamin, D.; Meineke, D.N.H.; D’ Este, E.; Kraemer, P.T.; Danzl, J.G.; Belov, V.N.; et al. Fluorescent Rhodamines and Fluorogenic Carbopyronines for Super-Resolution STED Microscopy in Living Cells. *Angew. Chem. Int. Ed.* **2016**, *55*, 3290–3294. [[CrossRef](#)] [[PubMed](#)]
27. Butkevich, A.N.; Belov, V.N.; Kolmakov, K.; Sokolov, V.V.; Shojaei, H.; Sidenstein, S.C.; Kamin, D.; Matthias, J.; Vlijm, R.; Engelhardt, J.; et al. Hydroxylated Fluorescent Dyes for Live-Cell Labeling: Synthesis, Spectra and Super-Resolution STED. *Chem. Eur. J.* **2017**, *23*, 12114–12119. [[CrossRef](#)]
28. Haynes, C.A.; Koder, R.L.; Miller, A.F.; Rodgers, D.W. Structures of Nitroreductase in Three States: Effects of Inhibitor Binding and Reduction. *J. Biol. Chem.* **2002**, *277*, 11513–11520. [[CrossRef](#)]
29. Horsman, M.R.; Mortensen, L.S.; Petersen, J.B.; Busk, M.; Overgaard, J. Imaging Hypoxia to Improve Radiotherapy Outcome. *Nat. Rev. Clin. Oncol.* **2012**, *9*, 674–687. [[CrossRef](#)]
30. Faraggi, M.; Peretz, P.; Rosenthal, I.; Weinraub, D. Solution Properties of Dye Lasers. Rhodamine B in Alcohols. *Chem. Phys. Lett.* **1984**, *103*, 310–314. [[CrossRef](#)]
31. Hinckley, D.A.; Seybold, P.G. A Spectroscopic/Thermodynamic Study of the Rhodamine B Lactone \rightleftharpoons Zwitterion Equilibrium. *Spectrochim. Acta A Mol. Biomol. Spectrosc.* **1988**, *44*, 1053–1059. [[CrossRef](#)]
32. Magde, D.; Rojas, G.E.; Seybold, P.G. Solvent Dependence of the Fluorescence Lifetimes of Xanthene Dyes. *Photochem. Photobiol.* **1999**, *70*, 737–744. [[CrossRef](#)]
33. Huth, B.G.; Farmer, G.I.; Kagan, M.R. Temperature-Dependent Measurements of a Flashlamp Pumped Dye Laser. *J. Appl. Phys.* **1969**, *40*, 5145–5147. [[CrossRef](#)]
34. Rosenthal, I.; Peretz, P.; Muszkat, K.A. Thermochromic and Hyperchromic Effects in Rhodamine B Solutions. *J. Phys. Chem.* **1979**, *83*, 350–353. [[CrossRef](#)]

35. Barigelletti, F. Effect of Temperature on the Photophysics of Rhodamine 101 in a Polar Solvent. *Chem. Phys. Lett.* **1987**, *140*, 603–606. [[CrossRef](#)]
36. Hinckley, D.A.; Seybold, P.G.; Borris, D.P. Solvatochromism and Thermochromism of Rhodamine Solutions. *Spectrochim. Acta A Mol. Biomol. Spectrosc.* **1986**, *42*, 747–754. [[CrossRef](#)]

Sample Availability: Samples of the compounds are not available from the authors.



© 2019 by the authors. Licensee MDPI, Basel, Switzerland. This article is an open access article distributed under the terms and conditions of the Creative Commons Attribution (CC BY) license (<http://creativecommons.org/licenses/by/4.0/>).